PLOS ONE

RESEARCH ARTICLE

The parametric study of hybrid nanofluid flow with heat transition characteristics over a fluctuating spinning disk

Xiao-Hong Zhang[1], Ebrahem A. Algehyne[2,3], Maryam G. Alshehri[2], Muhammad Bilal[4]*, Muhammad Altaf Khan[5], Taseer Muhammad[6]

1 College of Science, Hunan City University, Yiyangt, P. R. China, **2** Faculty of Science, Department of Mathematics, University of Tabuk, Tabuk, Saudi Arabia, **3** Nanotechnology Research Unit (NRU), University of Tabuk, Tabuk, Saudi Arabia, **4** Department of Mathematics, City University of Science and Information Technology, Peshawar, Pakistan, **5** Faculty of Natural and Agricultural Sciences, Institute for Groundwater Studies, University of the Free State, Bloemfontein, South Africa, **6** Department of Mathematics, College of Sciences, King Khalid University, Abha, Saudi Arabia

* bilalchd345@gmail.com

Citation: Zhang X-H, A. Algehyne E, G. Alshehri M, Bilal M, Khan MA, Muhammad T (2021) The parametric study of hybrid nanofluid flow with heat transition characteristics over a fluctuating spinning disk. PLoS ONE 16(8): e0254457. https://doi.org/10.1371/journal.pone.0254457

Editor: Oluwole Daniel Makinde, Stellenbosch University, SOUTH AFRICA

Received: May 28, 2021

Accepted: June 27, 2021

Published: August 16, 2021

Data Availability Statement: All the data used are inside the paper.

Funding: This study was funded by the Deanship of Scientific Research at King Khalid University, Abha, Saudi Arabia in the form of a grant to TM (GRP/342/42). Additionally, EA and MA received support from the University of Tabuk and EA received support from the Nanotechnology Research Unit (NRU), University of Tabuk, Saudi Arabia.

Abstract

The study explored the 3D numerical solution of an unsteady *Ag-MgO*/water hybrid nanofluid flow with mass and energy transmission generated by a wavy rotating disc moving up and down. The nanofluid is generated in the context of Ag-MgO nanomaterials. Magnesium oxide and silver nanoparticles have been heavily reported to have broad-spectrum antibacterial operations among metal oxides and metals. Silver nanoparticles are without a doubt the most commonly used inorganic nanoparticles, with numerous innovations in biomaterial's detection and antimicrobial operations. However, in current paper, the intention of the analysis is to boost thermal energy transmitting rates for a range of industrial implementations. When compared to a flat surface, energy transition is increased up to 15% due to the wavy swirling surface. The problem has been formulated as a system of PDEs, which included the Navier Stokes and Maxwell equations. Following that, the modeled equations are reduced to a dimensionless system of differential equations. The derived equations are then solved numerically using the Parametric Continuation Method (PCM). The findings are displayed graphically and debated. The geometry of a spinning disc is thought to have a positive impact on velocity and heat energy transfer. The insertion of nanostructured materials (silver and magnesium-oxide) increased the carrier fluid's thermal properties considerably. It is more effective at dealing with low energy transmission.

1. Introduction

Fluid flow over the substrate of a rotating disc has garnered considerable attention because of its consequences in real phenomena. Flow over the rotating disc surface is commonly used in electric power generation systems, co rotating machines, aerodynamics engineering, rotating equipment, geothermal sector, chemical reaction, and computer processing [1]. Accurate analysis and precise measurements of reaction are the prerequisite for better understanding the

Competing interests: The authors have declared that no competing interests exist.

factors that overcome kinetics of reaction. Electrode system of rotating disk is broadly used to examine the reactions kinetics and that are suffering from mass transmission deficiency [2]. Tassaddiq *et al.* [3] examined the MHD, an incompressible iron ferrite and carbon nanotubes CNTs hybrid nanoliquid over an impermeable spinning disk. They perceived that the fluid temperature and velocity are considerably increased by increasing disc rotating velocity. Mustafa *et al.* [4] used the Bingham fluid model to analyze the heat transmission and viscous dissipation for swirling viscoelastic fluid flow crossing over a permeable spinning disc. Using a greater suction velocity at the disc allows for a faster thermal efficiency. However, as the fluid yield stress increases, the heat transfer is expected to deteriorate. Hafeez and Khan [5] scrutinized the mass and heat flux theories in Oldroyd-B fluid flow over an extending disk. It should be noted that the solutal relaxation time coefficient has a negative impact on mass transmission rate. Gul *et al.* [6] modeled the hybrid nanofluid flow between disk and cone with several cases. Based on the analysis of the results, it was concluded that a rotating disc that a rotating disc with a fixed cone would attain the intended cooling of disk-cone tools if the surface temperature remains steady.

Fluid that is commonly used Ethanol, kerosene oil and water etc., which play a prominent role in energy transfer, heating and air conditioning processes, energy generation, and other small electronics mechanisms. However, since these liquids have a poor thermal energy transfer capacity, they are unable to accommodate the need for high heat exchange rates. Nanometer-sized particles (1-100nm), also recognized as nanomaterials, are applied to a natural fluid to substitute for this inadequacy and increase thermal conductivity. To quantify the thermophysical properties of various kinds of nanoparticles, the researcher used a variety of techniques [7]. Nanoparticles are used to clean surfaces in engineering because they have the ability to disperse and wet oil. It improves thermal efficiency, which is important in the fields of energy production, hypoxia, micro fabrication and metallurgy. Magnesium oxide MgO is a compound made up of Mg^{2+} and O^{2-} ions that are bonded together through a powerful ionic bond. It is made by calcination of $Mg\ (OH)^{2}$ and $MgCO^{3}$ at temperature range from 700˚C-1500˚C. Most of it is utilized in the hematologic and electrical industries. Similarly, Ag particles with antibacterial properties are used to control microorganism growth in wound, burns and surgical apparatus and infrastructure. Microorganisms are particularly toxic to compound based on silver and its ions. Hussanan *et al.* [8] investigated oxide nanomaterials in engine nanoliquids and water for energy up gradation. Using the finite element technique, Ghalambaz *et al.* [9] investigated convection flow of a hybrid nanofluid (Ag–MgO/water) within a cavity. Copper-Alumina micro materials were listed for the base fluid. Aluminum Oxide was used by Motlagh and Soltanpour [10] to elaborate the heat transition in a non-flat cavity. Acharya *et al.* [11] investigated the hybrid fluid flow over a spinning disc with the consequences of MHD and Hall current. They introduced the TiO_2 and Cu nanomaterials to creative a class of nanoliquid. The magnetic interaction on flow with CNTs nano powders via a porous tube is studied by Akber *et al.* [12]. Shah *et al.* [13] reported that an angled magnetic field, performance of copper selenide and the efficacy of chemical catalytic reactors effects the energy and concentration distribution of nanofluids. Sowmya *et al.* [14] uncovered natural convective thermal transference in a rectangular chamber with two heated fins on the bottom wall for a hybrid nanofluid flow employing iron oxide and silver nanomaterials. Zhou *et al.* [15] Khan addressed Von Karman's classic swirling flow for Maxwell fluid over a porous whirling disc with a constant suction/injection mechanism.

In the engineering sectors, complex nonlinear boundary value problems that cannot be addressed usually are often observed. Convergence is sensitive to the relaxation parameters and initial approach for many problems that are commonly solved by other numerical algorithms. The PCM's goal is to explore the method's generalizability as a feasible alternative to

nonlinear problems [16]. Shuaib *et al.* [17] emphasized the 3D unsteady fluid and heat propagation across the substrate of a non-flat stretchable rotating disc. The fluid has investigated under the effects of a magnetic strength from the outside. The feature of an ionic transition boundary layer flow over a gyrating disc was discovered by Shuaib *et al.* [18]. The Poisson's, Nernst-Planck equation and Navier Stokes equations, were used to solve for the ionic compounds. Wang *et al.* [19] presented stability analysis of nonlinear problems for engineering applications through parametric continuation algorithm. They also looked at the static bifurcation that happens when solving nonlinear initial value problems with different characteristic roots and provided an algorithm for instantly calculating the bifurcation points.

The aim of this study is to modify an idea of Ref. [20,21], by investigating the influence of two separate nanoparticles, Silver *Ag*/water and magnesium oxide *MgO*/water hybrid nanofluids, on a wavy spinning disc that moves upward and downward. This research is being considered in order to increase the thermal conductivity of the fluid flow. The modelled equations are solved numerically using the parametric continuation process (PCM), and the results have been validated and compared with Matlab's package boundary value solver (bvp4c). All outcomes are in the closest possible agreement with one another.

2. Mathematical formulation

The physical analysis of the problem, physicochemical characteristics and the equation of motion has been discussed in this section.

2.1 Physical description of the problem

We have assumed a 3D flow of *Ag-MgO*/Water (Silver and magnesium-oxide) hybrid nanoliquid over a wavy up and down moving spinning disk. Initially the disk is at $a(0) = h$. At a vertical distance $Z = a(t)$ the disk is moving with velocity $\omega = a(t)$. The consequences of buoyancy impacts are negligible. The disk is revolving about z-axis with angular velocity $\Omega(t)$, and it has been considered that the *Ag-MgO* nano-size particles are scattered consistent. The magnetic field of constant magnitude is uniformly applied with $\overrightarrow{B} = (B_r \overrightarrow{e}_r + B_\theta \overrightarrow{e}_\theta)$ and $B = \sqrt{B_r^2 + B_\theta^2}$ respectively, where $\overrightarrow{e}_r$ and $\overrightarrow{e}_\theta$ are unit vectors.

2.2 Equation of motion

The modeled equations, based on above presumption are expressed as [20,21]:

$$\frac{\partial u}{\partial r} + \frac{\partial w}{\partial z} + \frac{u}{r} = 0, \tag{1}$$

$$\rho_{hnf}\left(\frac{\partial u}{\partial t} + u\frac{\partial u}{\partial r} + w\frac{\partial u}{\partial z} - \frac{v^2}{r}\right) = -\frac{\partial p}{\partial r} + \mu_{hnf}\left(\frac{\partial^2 u}{\partial r^2} + \frac{\partial^2 u}{\partial z^2} + \frac{1}{r}\frac{\partial u}{\partial r} - \frac{u}{r^2}\right) + F_r, \tag{2}$$

$$\rho_{hnf}\left(\frac{\partial v}{\partial t} + u\frac{\partial v}{\partial r} + w\frac{\partial v}{\partial z} - \frac{uv}{r}\right) = \mu_{hnf}\left(\frac{\partial^2 v}{\partial r^2} + \frac{\partial^2 v}{\partial z^2} + \frac{1}{r}\frac{\partial v}{\partial r} - \frac{v}{r^2}\right), \tag{3}$$

$$\rho_{hnf}\left(\frac{\partial w}{\partial t} + u\frac{\partial w}{\partial r} + w\frac{\partial w}{\partial z}\right) = -\frac{\partial p}{\partial r} + \mu_{hnf}\left(\frac{\partial^2 w}{\partial r^2} + \frac{\partial^2 w}{\partial z^2} + \frac{1}{r}\frac{\partial w}{\partial r}\right) + F_\theta, \tag{4}$$

$$\left(\frac{\partial T}{\partial t} + u\frac{\partial T}{\partial r} + w\frac{\partial T}{\partial z}\right) = \frac{k}{(\rho C_p)_{hnf}}\left(\frac{\partial^2 T}{\partial r^2} + \frac{1}{r}\frac{\partial T}{\partial r} + \frac{\partial^2 T}{\partial z^2}\right), \tag{5}$$

$$\left(\frac{\partial B_r}{\partial t}\right) = -w\frac{\partial B_r}{\partial z} - Br\frac{\partial B_w}{\partial z} + u\frac{\partial B_z}{\partial z} + Bz\frac{\partial u}{\partial z} + \frac{1}{\sigma\mu}\left(\frac{\partial^2 B_r}{\partial r^2} + \frac{\partial^2 B_r}{\partial z^2} + \frac{1}{r}\frac{\partial B_r}{\partial r} - \frac{Br}{r^2}\right), \tag{6}$$

$$\left(\frac{\partial B_z}{\partial t}\right) = w\frac{\partial B_r}{\partial r} + Br\frac{\partial B_w}{\partial r} + \frac{1}{r}wBr - u\frac{\partial B_z}{\partial r} - Bz\frac{\partial u}{\partial r} - \frac{1}{r}uBz + \frac{1}{\sigma\mu}\left(\frac{\partial^2 B_z}{\partial r^2} + \frac{\partial^2 B_z}{\partial z^2} + \frac{1}{r}\frac{\partial B_z}{\partial r}\right), \tag{7}$$

Here F_r and F_θ along x and z direction are the body forces, respectively, which can be stated as [21]:

$$F_r = \frac{Ha^2\mu_{hnf}}{R^2}(v\sin\theta\cos\theta - u\sin^2\theta), \tag{8}$$

$$F_\theta = \frac{Ha^2\mu_{hnf}}{R^2}(u\sin\theta\cos\theta - v\sin^2\theta), \tag{9}$$

Here, Ha is $LB_0\sqrt{\frac{\sigma}{\mu}}$, in which θ is the direction and B_0 is the magnitude of magnetic field, where the velocity components are specified as u,v,w.

2.3 Boundary condition

The initial and boundary conditions for wavy gyrating disk are:

$$u = 0,\ v = r\Omega_0(t),\ w = w_0(t),\ T = T_0,\ Br = 0,\ Bz = 0 \text{ at } z = 0$$

$$u\overrightarrow{0},\ v\overrightarrow{0},\ w\overrightarrow{0},\ T\overrightarrow{T_\infty},\ Br = \frac{M_0}{2R}, Bz = -\alpha M_0 \text{ at } z\overrightarrow{\infty}. \tag{10}$$

2.4 Thermophysical properties of nanoliquid

The density and specific heat capacity of the hybrid nanofluid can be revealed as [21]:

$$\rho_{hnf} = \left\{(1-\varphi_2)\left[(1-\varphi_1)_{\rho_f} + \varphi_1\rho_{s1}\right]\right\} + \varphi_2\rho_{s2}, \tag{11}$$

$$(\rho C_p)_{hnf} = \left\{(1-\varphi_2)\left[(1-\varphi_1)(\rho C_p)_f + \varphi_1(\rho C_p)_{s1}\right]\right\} + \varphi_2(\rho C_p)_{s2}, \tag{12}$$

where $(C_p)_{s1}$,$(C_p)_{s2}$ are specific heat capacity, ρ_{s1},ρ_{s2} are the density and φ_1,φ_2 are the volume friction of the *Ag-MgO* hybrid nanoliquid respectively shown in Table 1.

The hybrid nanofluid viscosity μ_{hnf} is expressed as [22]:

$$\frac{\mu_{hnf}}{\mu_{bf}} = \frac{1}{(1-\varphi_1)^{2.5}(1-\varphi_2)^{2.5}}, \tag{13}$$

Here, the thermal conductivity and Prandtl number is expressed as [21]:

$$k_{hnf} = -\frac{q_w}{\partial\theta/\partial y},\ \mathrm{Pr}_{hnf} = \frac{(\mu C_p)_{hnf}}{k_{hnf}}. \tag{14}$$

Table 1. The numerical properties of water and hybrid nanofluid [20].

	ρ(kg/m^3)	C_p(j/kgK)	k(W/mK)	$\beta\times10^5(K^{-1})$
Pure water	997.1	4179	0.613	21
Magnesium oxide	3560	955	45	1.80
Silver	10,500	235	429	1.89

https://doi.org/10.1371/journal.pone.0254457.t001

2.5 Karman's approach

We use the following similarity framework, to reduce Eqs (1)–(7) and (10) to the system of ODEs [20]:

$$u=\frac{r\nu}{a^2(t)}f(\eta),\ v=\frac{r\nu}{a^2(t)}g(\eta),\ w=\frac{\nu}{a(t)}h(\eta),\ p=\frac{p\nu^2}{a^2(t)}p(\eta),\ Br=\frac{r\Omega M_0}{a(t)}m'(\eta),$$

$$Bz=\frac{M_0(2\nu_f\Omega)^{1/2}}{a(t)}n(\eta),\ T=T_\infty+\Delta T_\infty,\ \eta=\frac{Z}{a(t)}-1,\ \eta_Z=\frac{1}{a(t)},\ \eta_t=\frac{-a(t)}{a(t)}(\eta+1). \quad (15)$$

As a result of Eq (15), we get the following:

$$f^{''}=\frac{\rho_{hnf}}{\mu_{hnf}}\left(hf'+f^2-g^2-S\frac{(\eta+1)f'}{2}+f\right)+A\omega(g\sin\theta\cos\theta-f\sin^2\theta), \quad (16)$$

$$g^{''}=\frac{\rho_{hnf}}{\mu_{hnf}}\left(hg'+2fg-S\left(\frac{(\eta+1)g'}{2}-g\right)\right), \quad (17)$$

$$h^{''}=\frac{\rho_{hnf}}{\mu_{hnf}}\left(hh'-S\frac{(\eta+1)h'}{2}+h'\right)-A\omega(f\sin\theta\cos\theta-g\sin^2\theta), \quad (18)$$

$$\theta^{''}=\rho_{hnf}\left(h\theta'-S\left(\frac{(\eta+1)\theta'}{2}+\gamma\theta\right)\right), \quad (19)$$

$$m^{'''}=Bt\left(-hm^{''}+m'h'+fn'+nf'+S\left(\frac{m^{''}\eta}{2}+m'\right)\right), \quad (20)$$

$$n^{''}=-Bt\left(2hm'+2nf-\frac{S}{2}(n'\eta+n)\right). \quad (21)$$

The transform conditions are:

$$f(0)=0,\ h(0)=\beta\frac{S}{2},\ g(0)=\omega,\theta(0)=m'(0)=n(0)=1 \text{ at } \eta=0,$$

$$f(\eta)\overrightarrow{0},\ g(\eta)\overrightarrow{0},\ h(\eta)\overrightarrow{0},\ \theta(\eta)\overrightarrow{0},\ m'(\eta)\overrightarrow{0},n(\eta)\overrightarrow{0},\ \text{as } \eta=\infty, \quad (22)$$

Sign ω edify disk's rotation, S controlled the up and down fluctuating of the disk and γ is the is the thermal energy parameter, which can be defined as [18]:

$$S = 2\frac{a^*(t)a(t)}{\nu},\ \omega = 2\frac{a^2(t)\Omega(t)}{\nu},\ \gamma = \frac{1}{2}\frac{a(t)T}{a^*(t)\Delta T}. \tag{23}$$

The dimensionless form of skin friction and Nusselt number is:

$$C_f = \frac{\sqrt{\tau_{wr}^2 - \tau_{w\phi}^2}}{\rho_f(\Omega r)^2} \text{ and } Nu = \frac{rq_w}{k_f(T_w - T_\infty)}. \tag{24}$$

Where, τ_{wr} and $\tau_{w\phi}$ represent the radial and transverse stress respectively.

3. Numerical solution

The following steps have been used, while solving the system of ODE (16–21) and their boundary conditions (22):

Step 1: Reducing the system of modeled equations to the first order ODEwe introduced the following similarity variables:

$$\left.\begin{aligned} &\chi_1(\eta) = f(\eta),\ \ \chi_2(\eta) = f'(\eta),\ \ \chi_3(\eta) = g(\eta),\\ &\chi_4(\eta) = g'(\eta),\ \ \chi_5(\eta) = h(\eta),\ \ \chi_6(\eta) = h'(\eta),\\ &\chi_7(\eta) = \theta(\eta),\ \ \chi_8(\eta) = \theta'(\eta),\ \ \chi_9(\eta) = m(\eta),\\ &\chi_{10}(\eta) = m'(\eta),\ \ \chi_{11}(\eta) = m''(\eta),\ \ \chi_{12}(\eta) = n(\eta),\\ &\chi_{13}(\eta) = n'(\eta), \end{aligned}\right\} \tag{25}$$

Using Eq (25) into the BVP (16–21) and (22), we get:

$$\begin{aligned} \chi_2'(\eta) = &\frac{\rho_{hnf}}{\mu_{hnf}}\left(\left(\chi_5(\eta) - S\frac{(\eta+1)}{2}\right)\chi_2(\eta) + (\chi_1(\eta))^2 - (\chi_3(\eta))^2 - S\chi_1(\eta)\right)\\ &+A\omega(\chi_3(\eta)\sin\theta\cos\theta - \chi_1(\eta)\sin^2\theta) \end{aligned} \tag{26}$$

$$\chi_4'(\eta) = \frac{\rho_{hnf}}{\mu_{hnf}}\left(\left(\chi_5(\eta) - S\frac{(\eta+1)}{2}\right)\chi_4(\eta) + 2\chi_1(\eta)\chi_3(\eta) - S\chi_3(\eta)\right) \tag{27}$$

$$\chi_6'(\eta) = \frac{\rho_{hnf}}{\mu_{hnf}}\left(\left(\chi_5(\eta) - S\frac{(\eta+1)}{2} + 1\right)\chi_6(\eta)\right) - A\omega(\chi_1(\eta)\sin\theta\cos\theta - \chi_3(\eta)\sin^2\theta) \tag{28}$$

$$\chi_8'(\eta) = \rho_{hnf}\left(\left(\chi_5(\eta) - S\frac{(\eta+1)}{2}\right)\chi_8(\eta) - S\chi_7\gamma(\eta)\right) \tag{29}$$

$$\chi_{11}'(\eta) = Bt\left(\left(-\chi_5(\eta) - \frac{S\eta}{2}\right)\chi_{11}(\eta) + S\chi_{10}(\eta) + \chi_{10}(\eta)\chi_6(\eta) + \chi_1(\eta)\chi_{13}(\eta) + \chi_{13}(\eta)\chi_2(\eta)\right) \tag{30}$$

$$\chi_{13}'(\eta) = -Bt\left(-\frac{S}{2}(\eta\chi_{13}(\eta) + \chi_{12}(\eta))2\chi_1(\eta)\chi_{12}(\eta) + 2\chi_5(\eta)\chi_{10}(\eta)\right) \tag{31}$$

the boundary conditions are:

$$\chi_1(\eta)=0,\ \chi_3(\eta)=\omega,\ \chi_5(\eta)=\beta\frac{S}{2},\ \chi_7(\eta)=\chi_{10}(\eta)=\chi_{12}(\eta)=1\ at\ \eta=0,$$
$$\chi_1(\eta)\overrightarrow{0},\ \chi_3(\eta)\overrightarrow{0},\ \chi_5(\eta)\overrightarrow{0},\ \chi_7(\eta)\overrightarrow{0},\ \chi_{10}(\eta)\overrightarrow{0},\ \chi_{12}(\eta)\overrightarrow{0}\ at\ \eta\overrightarrow{\infty}. \tag{32}$$

Step 2: **By introducing the embedding parameter p**

We introduced the parameter p in the above system of Eqs (26–31) as follow:

$$\chi_2{}'(\eta)=\frac{\rho_{hnf}}{\mu_{hnf}}\left(\left(\chi_5(\eta)-S\frac{(\eta+1)}{2}\right)(\chi_2(\eta)-1)p+(\chi_1(\eta))^2-(\chi_3(\eta))^2-S\chi_1(\eta)\right)$$
$$+A\omega(\chi_3(\eta)\sin\theta\cos\theta-\chi_1(\eta)\sin^2\theta) \tag{33}$$

$$\chi_4{}'(\eta)=\frac{\rho_{hnf}}{\mu_{hnf}}\left(\left(\chi_5(\eta)-S\frac{(\eta+1)}{2}\right)(\chi_4(\eta)-1)p+2\chi_1(\eta)\chi_3(\eta)-S\chi_3(\eta)\right) \tag{34}$$

$$\chi_6{}'(\eta)=\frac{\rho_{hnf}}{\mu_{hnf}}\left(\left(\chi_5(\eta)-S\frac{(\eta+1)}{2}+1\right)(\chi_6(\eta)-1)p\right)$$
$$-A\omega(\chi_1(\eta)\sin\theta\cos\theta-\chi_3(\eta)\sin^2\theta) \tag{35}$$

$$\chi_8{}'(\eta)=\rho_{hnf}\left(\left(\chi_5(\eta)-S\frac{(\eta+1)}{2}\right)(\chi_8(\eta)-1)p-S\chi_7\gamma(\eta)\right) \tag{36}$$

$$\chi_{11}{}'(\eta)=Bt\left(\left(-\chi_5(\eta)-\frac{S\eta}{2}\right)(\chi_{11}(\eta)-1)p+S\chi_{10}(\eta)+\chi_{10}(\eta)\chi_6(\eta)\right)$$
$$+(+\chi_1(\eta)\chi_{13}(\eta)+\chi_{13}(\eta)\chi_2(\eta)) \tag{37}$$

$$\chi_{13}{}'(\eta)=-Bt\left(-\frac{S}{2}(\eta\chi_{13}(\eta)+(\chi_{12}(\eta)-1)p)2\chi_1(\eta)\chi_{12}(\eta)+2\chi_5(\eta)\chi_{10}(\eta)\right) \tag{38}$$

Step 3: **Differentiating w.r.t parameter 'p'**

Eqs (33–38) after differentiating w.r.t parameter p reform to the following structure with respect to parameter p

$$V'=AV+R, \tag{39}$$

where, R is the remainder and A is the coefficient matrix:

$$\frac{d\chi_i}{d\tau} \tag{40}$$

where i = 1, 2, ... .11.

Step 4: Apply specify Cauchy problem and superposition principle for each component

$$V=aU+W, \tag{41}$$

where U, W are unknown vector functions and a is unknown blend coefficient. Solving the

Cauchy problems for each component

$$U' = aU, \tag{42}$$

$$W' = AW + R, \tag{43}$$

by putting Eq (41) into the original Eq (39), we get

$$(aU + W)' = A(aU + W) + R, \tag{44}$$

Step **5: Solving the Cauchy problems**

The numerical implicit scheme is implemented in the proposed problem, presented as follow: From Eqs (42) and (43)

$$\frac{U^{i+1} - U^i}{\Delta\eta} = AU^{i+1}, \ or \ (I - \Delta\eta A)U^{i+1} = U^i, \tag{45}$$

$$\frac{W^{i+1} - W^i}{\Delta\eta} = AW^{i+1}, \ or \ (I - \Delta\eta A)W^{i+1} = W^i, \tag{46}$$

here, we obtained the iterative form of the problem.

$$U^{i+1} = (I - \Delta\eta A)^{-1}U^i, \tag{47}$$

$$W^{i+1} = (I - \Delta\eta A)^{-1}(W^i + \Delta\eta R). \tag{48}$$

4. Analysis and discussion of results

4.1 Analysis

The numerical outcomes of the system of DE (Differential Equations) are calculated via using PCM, and the bvp4c technique has been used to compare and validate the results. The results have been revealed through Figs (2–11). Fig 1 displays the mechanism of fluid flow over a curvy surface with up and down fluctuation under the consequences of magnetic field. In current paper, the intention of the analysis is to boost the thermal energy transmitting rates for a range of industrial implementations. When compared to a flat surface, energy transition is increased up to 15% due to the wavy swirling surface.

4.2 Discussion of results

Figs (2–5) elaborate the upshot of volume friction parameters (ϕ_1 or ϕ_{Ag} and ϕ_2 or ϕ_{MgO}) on axial velocity $f(\eta)$ and energy profile $\theta(\eta)$ respectively. It can be perceived that the velocity and temperature transmission rate enhance with the rising values of ϕ_1&ϕ_2. Physically, the increasing number of nanoparticles (*Ag-MgO*) in base fluid reduces the specific heat capacity of water and improve the thermal diffusivity, because the specific heat capacity of silver and magnesium-oxide is less than water. Eventually, fluid losses its viscosity, which cause rises in temperature and velocity of fluid.

The unsteadiness parameter S upshot on axial $f(\eta)$ and azimuthal velocity $h(\eta)$ profiles is demonstrated through Figs 6 & 7, respectively. It has been concluded that the axial velocity enhances with the positive increment of unsteadiness parameter S, while azimuthal velocity reduces. Because the kinetic viscosity of fluid deceases with its effect, that's why such scenario has been observed in Fig 6. The effects of disk rotation ω parameter on radial velocity $g(\eta)$ is shown via Fig 8.

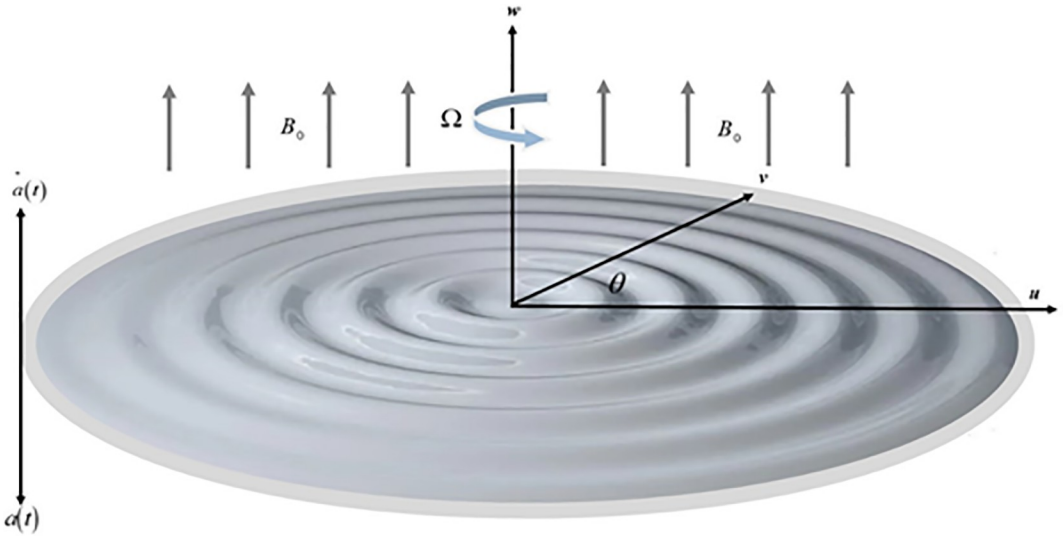

Fig 1.

https://doi.org/10.1371/journal.pone.0254457.g001

It's reasonable to assume that improvement rate of disk rotation significantly encourages the kinematic energy of the fluid ions, that leads to an increase in velocity $g(\eta)$, which also generates heat. The disc surface eventually heats up and improves the fluid temperature $\theta(\eta)$. Fig 9 revealed that the effect of parameter γ reduces the temperature profile. Because the fluid particle releases thermal energy during upward/downward movement, which causes the declination of fluid temperature. The rotating disk's upward and downward velocity is regulated by the parameter γ.

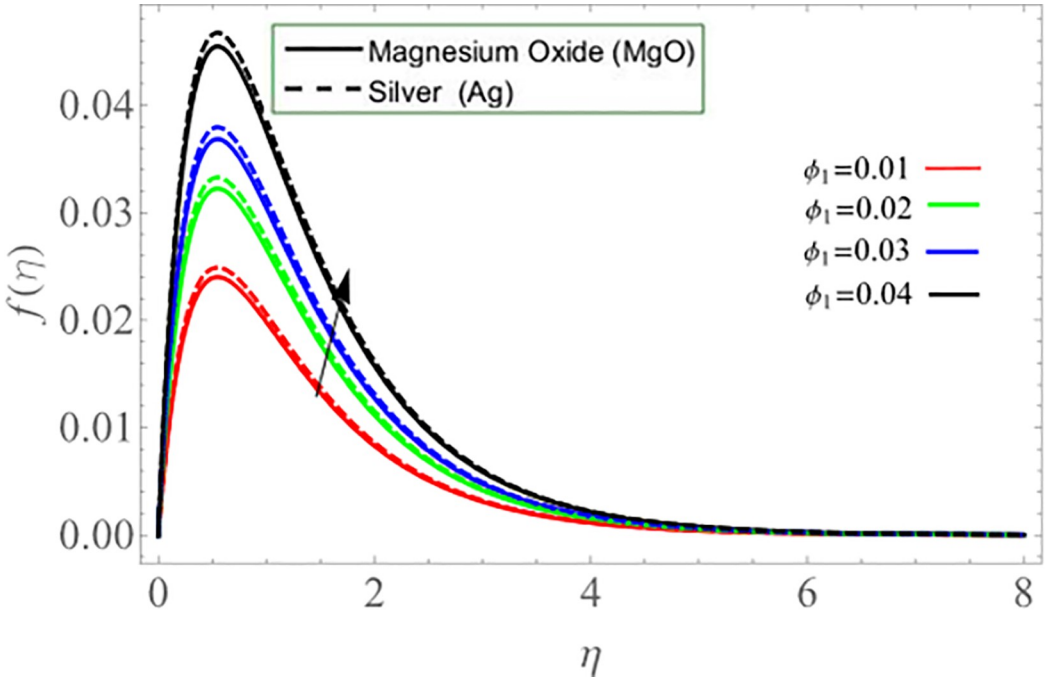

Fig 2.

https://doi.org/10.1371/journal.pone.0254457.g002

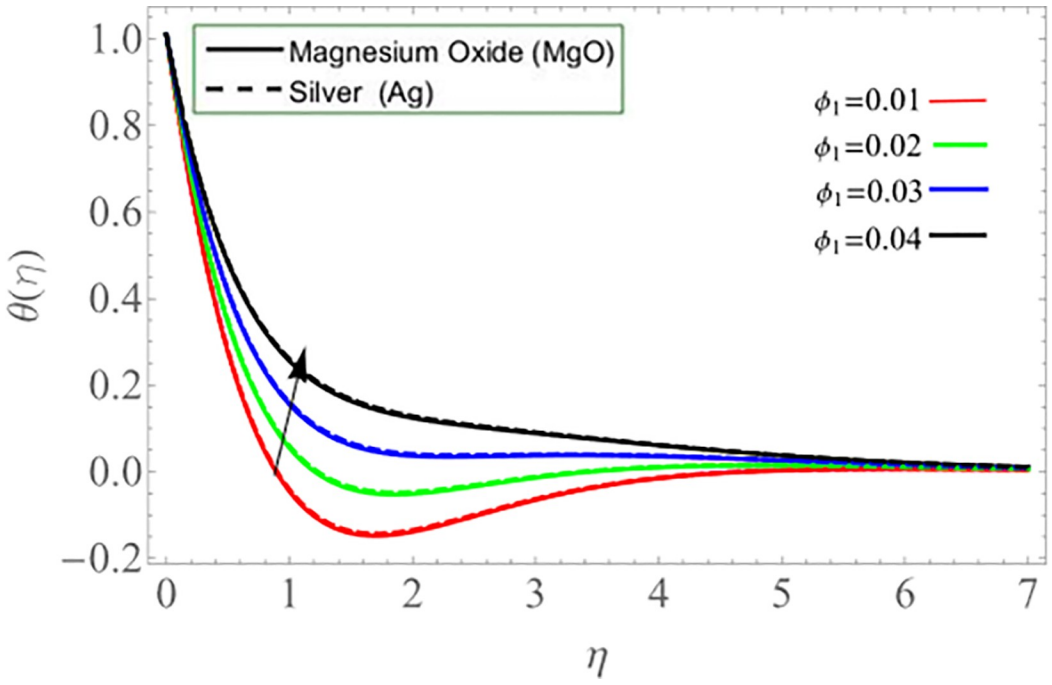

Fig 3.

https://doi.org/10.1371/journal.pone.0254457.g003

Fig 10 explored the consequences of Prandtl number *Pr* on energy profile. It can be noticed that the temperature declines by the action of Prandtl number. Physically, the action of Prandtl number directly affect the dynamic viscosity and specific heat capacity of fluid, as result the

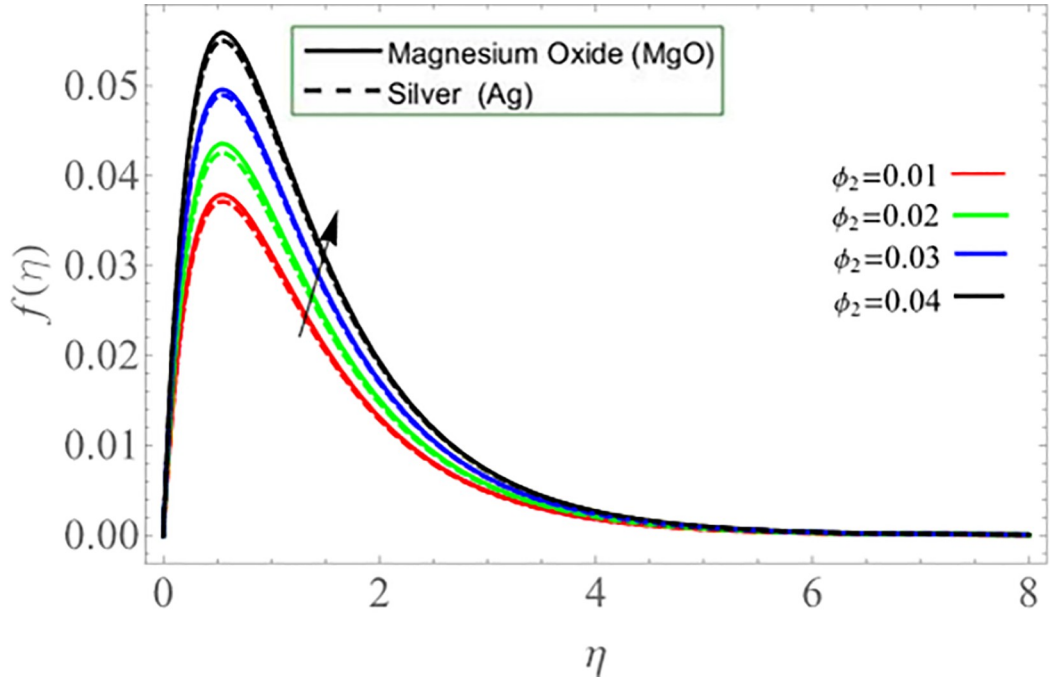

Fig 4.

https://doi.org/10.1371/journal.pone.0254457.g004

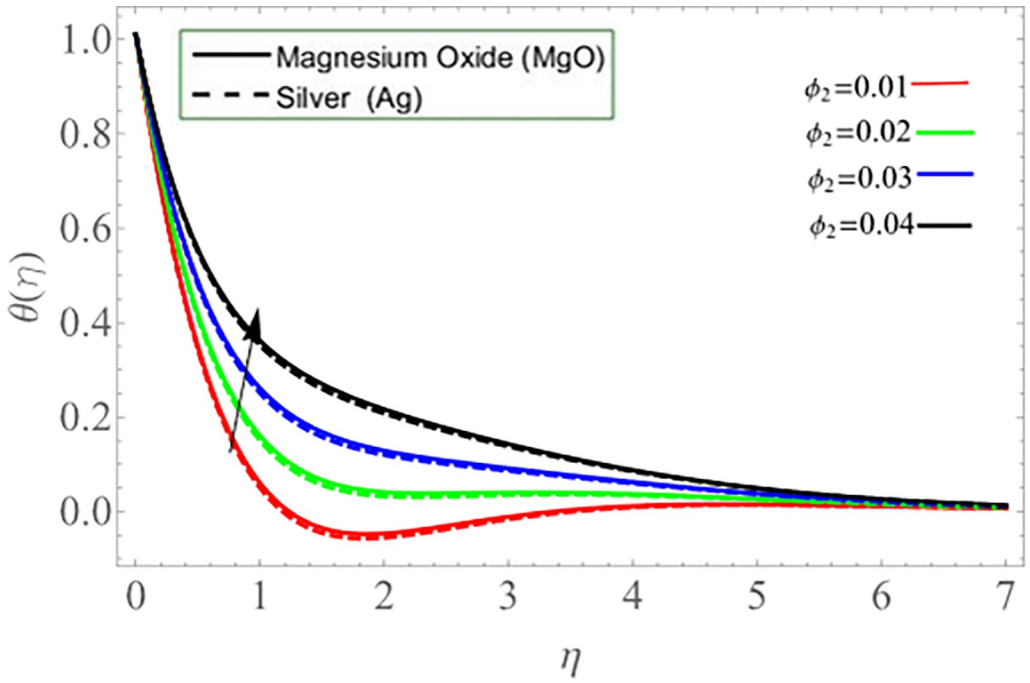

Fig 5.

https://doi.org/10.1371/journal.pone.0254457.g005

fluid thermal capability declines. Figs 11 & 12 demonstrate the influence of Batchlor number *Bt* on magnetic strength profile along axial $m'(\eta)$ and radial direction $n(\eta)$, respectively. The magnetic strength profile show declination versus the influence of Batchlor number, because the increment in *Bt* negatively affect the molecular diffusion rate of fluid.

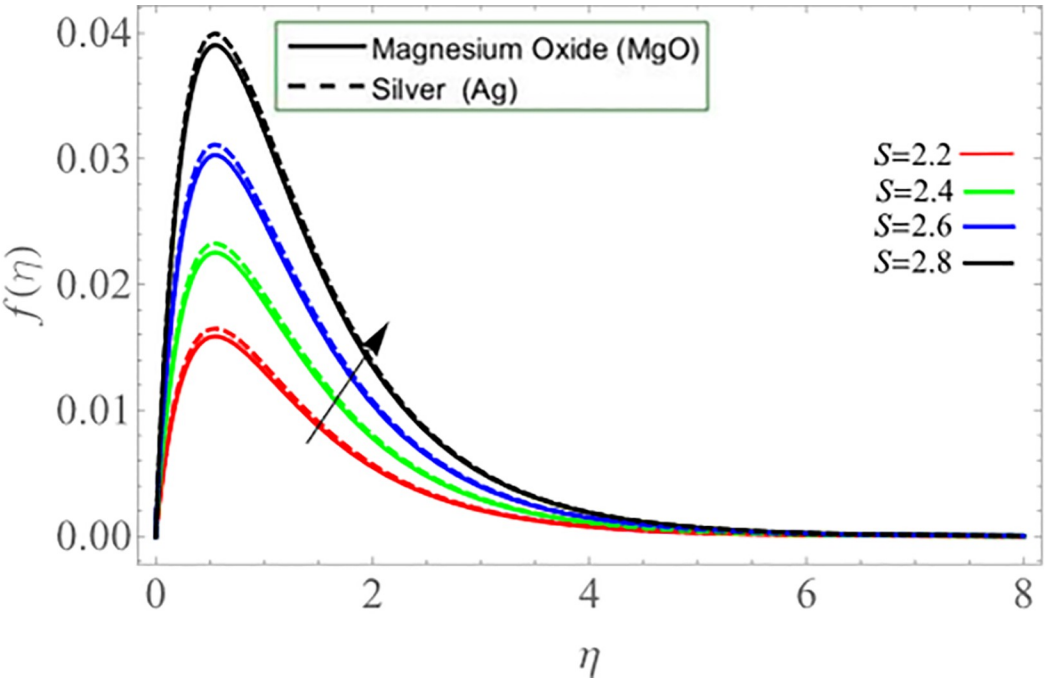

Fig 6.

https://doi.org/10.1371/journal.pone.0254457.g006

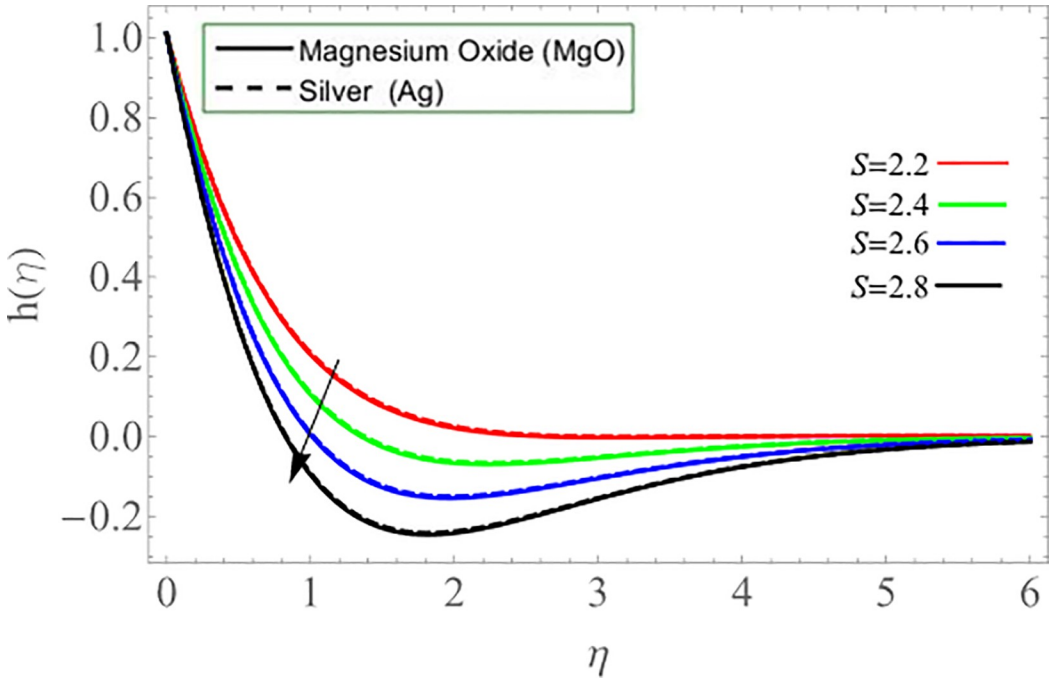

Fig 7.

https://doi.org/10.1371/journal.pone.0254457.g007

Table 1 elaborate the thermophysical characteristics of silver, base fluid, and magnesium-oxide. Table 2 revealed the comparison between PCM and bvp4c method numerically for all velocities. It can be presumed that the parametric continuation method has strong convergence versus other numerical method. Tables 3 and 4 display the influence of nanoparticles quantity ϕ on velocity radial and azimuthal direction, skin fraction and Nusselt number.

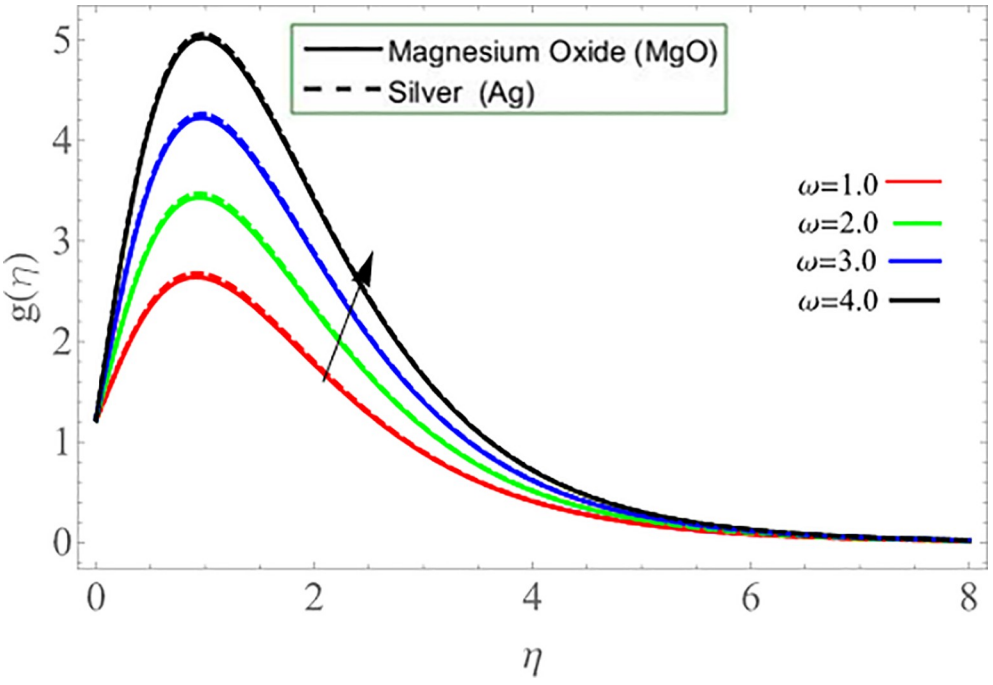

Fig 8.

https://doi.org/10.1371/journal.pone.0254457.g008

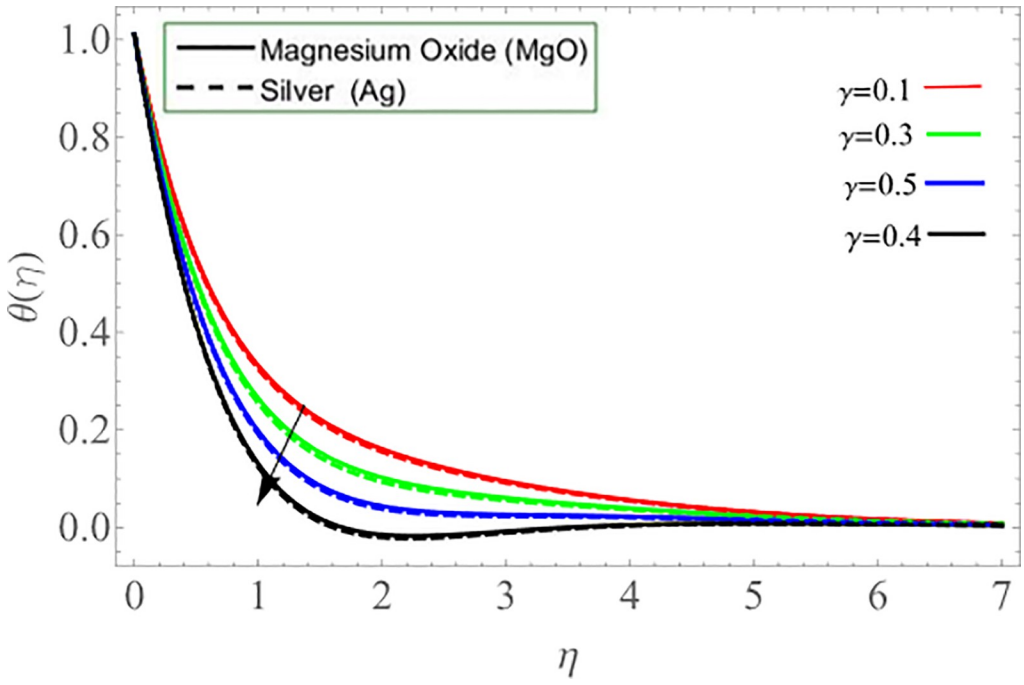

Fig 9.

https://doi.org/10.1371/journal.pone.0254457.g009

5. Conclusion

In the present study, we numerically scrutinized an unsteady 3D numerical model for *Ag-MgO* hybrid nanoliquid flow with mass and energy transition caused by the up and downward

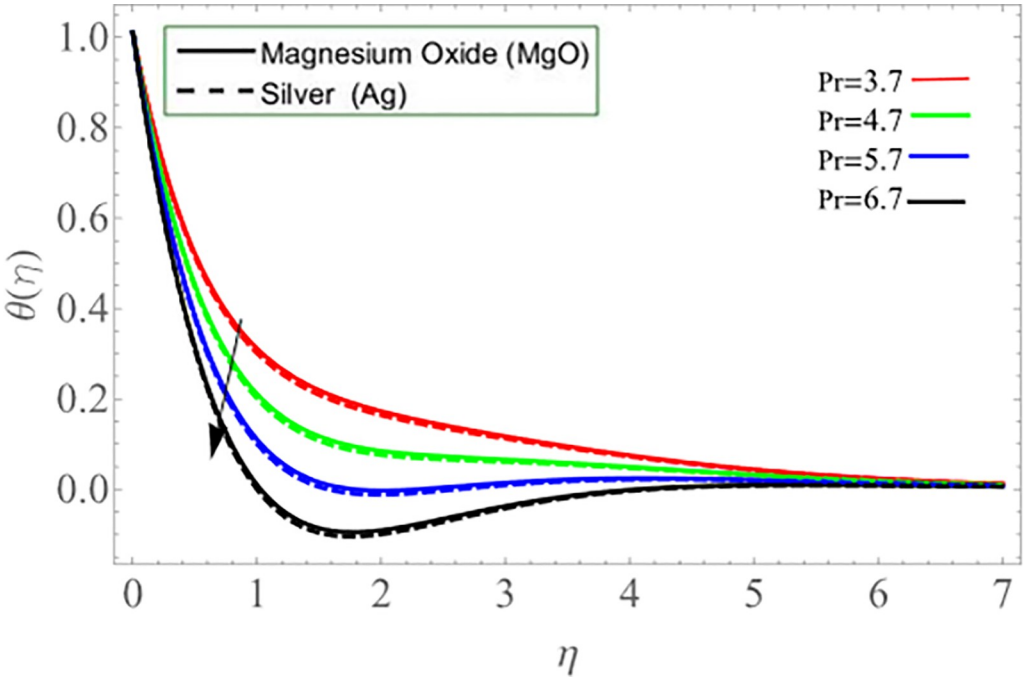

Fig 10.

https://doi.org/10.1371/journal.pone.0254457.g010

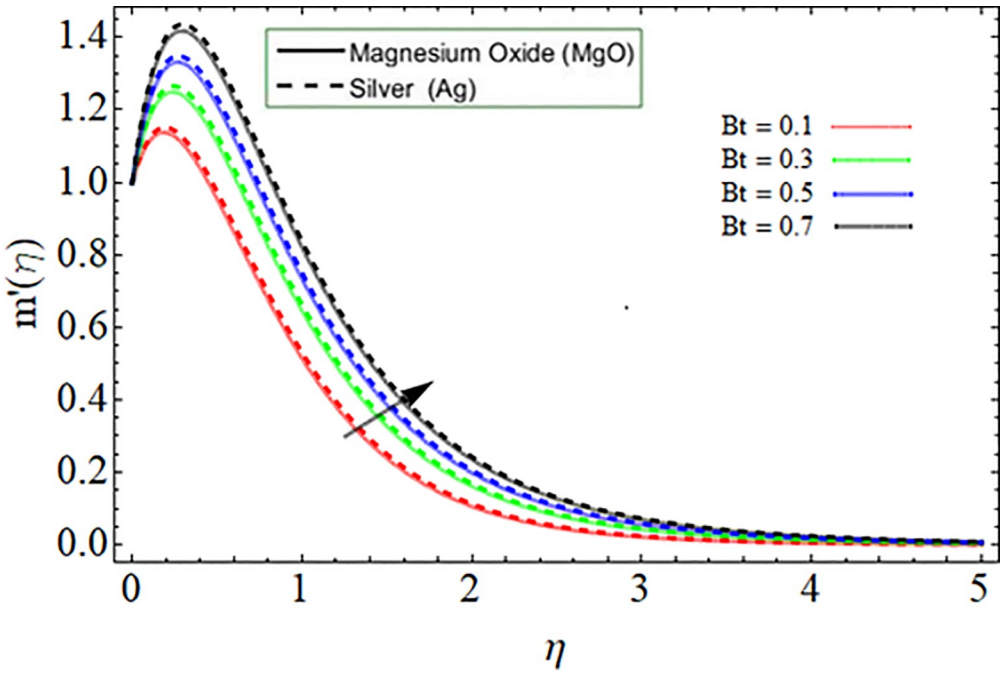

Fig 11.

https://doi.org/10.1371/journal.pone.0254457.g011

fluctuation of a wavy gyrating disc. Magnesium oxide and silver nanoparticles have been heavily reported to have broad-spectrum antibacterial operations among metal oxides and metals. However, in current paper, the study's goal is to increase the rate of thermal energy propagation for a variety of industrial applications. For the purpose, the problem has been

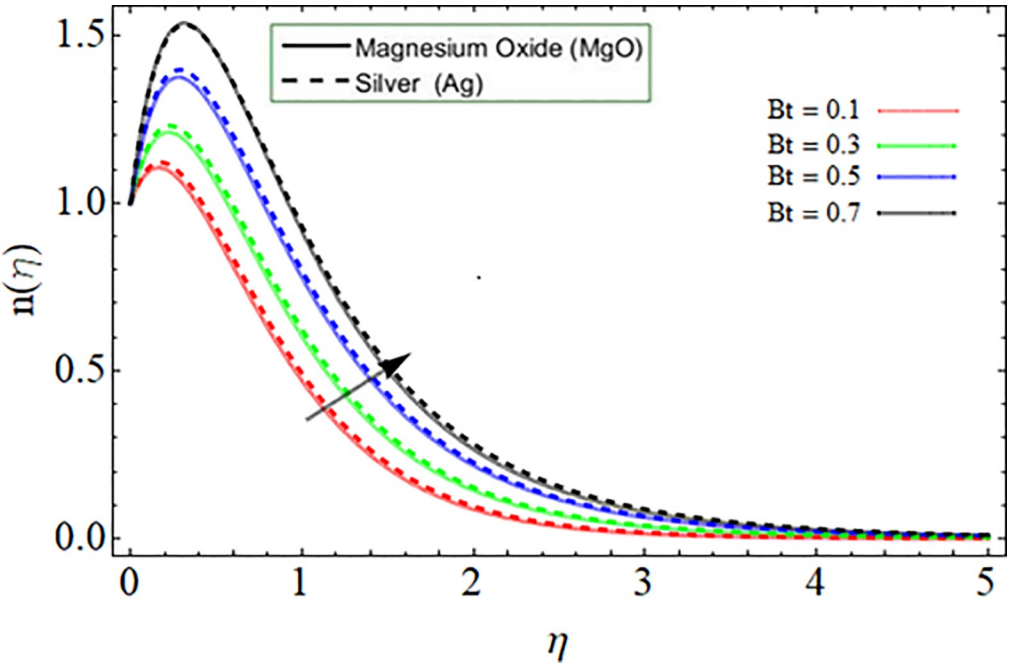

Fig 12.

https://doi.org/10.1371/journal.pone.0254457.g012

Table 2. Comparative analysis between PCM and bvp4c method.

	PCM			bvp4c		
η	$f(\eta)$	$g(\eta)$	$\theta(\eta)$	$f(\eta)$	$g(\eta)$	$\theta(\eta)$
0.0	0.0000	0.0000	1.0000	0.0000	0.0000	1.0000
0.5	0.0002	0.0020	0.2711	0.0002	0.0020	0.2721
1.0	0.0060	0.0157	0.0572	0.00061	0.01488	0.0572
1.5	-0.0391	-0.0771	0.0093	-0.0393	-0.0775	0.0097
2.0	-0.1359	-0.1913	0.0019	-0.1360	-0.1914	0.0008

https://doi.org/10.1371/journal.pone.0254457.t002

Table 3. The comparative analysis of silver and magnesium-oxide nanoparticles on velocity profile.

	Silver (Ag)		Magnesium oxide *MgO*	
η	$f'(0)$	$g'(0)$	$f'(0)$	$g'(0)$
0.00	1.3725	1.5912	1.4323	1.6562
0.05	1.5134	1.6724	1.8735	1.7821
0.01	1.7642	1.8054	2.1012	1.8922
0.15	2.0400	2.1791	2.2700	1.2901
0.20	2.2531	2.3753	2.4531	2.5102

https://doi.org/10.1371/journal.pone.0254457.t003

Table 4. Quantitively analysis for Nusselt number and Skin fraction.

	Silver (Ag)		Magnesium oxide *MgO*	
η	$h'(0)$	$\theta'(0)$	$h'(0)$	$\theta'(0)$
0.00	1.2724	1.6954	1.5513	1.6582
0.05	1.2921	1.4362	1.3835	1.7734
0.10	1.5139	1.2482	0.1012	1.7622
0.15	0.3612	1.7014	1.3910	2.3684

https://doi.org/10.1371/journal.pone.0254457.t004

formulated as a system of partial differential equations (Navier Stokes and Maxwell). During the study, the following observation have been made:

- Silver nanoparticles are without a doubt the most used inorganic nanoparticles, with numerous innovations in biomaterial's detection and antimicrobial operations.
- In comparison to a smooth substrate the wavy spinning surface raises the heat transfer rate by 15%.
- Magnesium oxide (MgO) is made up of Mg^{2+} and O^{2-} ions that are held together by a strong ionic bond. Which can be synthesized at temperatures ranging from 700 ^{0}C to 1500 ^{0}C degrees Celsius and is primarily used in refractory and electrical applications.
- The up and downward fluctuation of the curly spinning disc affects fluid temperature and velocity in a constructive way.
- Water's thermophysical properties are improved by the close bonds between water atoms (H^++OH^-) and silver ions Ag^+.
- Hybrid nanoliquids are more effective at overcoming low energy transfer. For example, it improves carrier fluid thermal efficiency, which is essential in power generation, microfabrication, hyperthermia, metallurgical fields and air conditioning.

- The parametric continuation method is a strong numerical technique for highly nonlinear system of PDE than others numerical algorithm.

Acknowledgments

The second and third authors would like to acknowledge the support provided by the University of Tabuk. Furthermore, the second author would like to acknowledge the support provided by the Nanotechnology Research Unit (NRU), University of Tabuk, Saudi Arabia.

Author Contributions

Conceptualization: Xiao-Hong Zhang, Maryam G. Alshehri, Taseer Muhammad.

Data curation: Ebrahem A. Algehyne, Taseer Muhammad.

Formal analysis: Xiao-Hong Zhang, Maryam G. Alshehri.

Funding acquisition: Xiao-Hong Zhang.

Investigation: Muhammad Bilal.

Methodology: Ebrahem A. Algehyne.

Project administration: Maryam G. Alshehri, Taseer Muhammad.

Resources: Xiao-Hong Zhang, Ebrahem A. Algehyne, Taseer Muhammad.

Software: Ebrahem A. Algehyne, Taseer Muhammad.

Supervision: Muhammad Altaf Khan.

Validation: Ebrahem A. Algehyne, Maryam G. Alshehri, Muhammad Altaf Khan.

Visualization: Xiao-Hong Zhang, Ebrahem A. Algehyne, Maryam G. Alshehri, Taseer Muhammad.

Writing – original draft: Muhammad Bilal.

Writing – review & editing: Xiao-Hong Zhang, Ebrahem A. Algehyne, Maryam G. Alshehri, Muhammad Bilal, Taseer Muhammad.

References

1. Ahmadian A., Bilal M., Khan M. A., & Asjad M. I. (2020). The non-Newtonian maxwell nanofluid flow between two parallel rotating disks under the effects of magnetic field. *Scientific Reports*, 10(1), 1–14. https://doi.org/10.1038/s41598-019-56847-4 PMID: 31913322
2. Chen W., Xu M. L., Li M. F., Wei Z., Cai J., & Chen Y. X. (2020). Quantifying intrinsic kinetics of electrochemical reaction controlled by mass transfer of multiple species under rotating disk electrode configuration. *Journal of Electroanalytical Chemistry*, 872, 114042.
3. Tassaddiq A., Khan S., Bilal M., Gul T., Mukhtar S., Shah Z., et al. (2020). Heat and mass transfer together with hybrid nanofluid flow over a rotating disk. *AIP Advances*, 10(5), 055317.
4. Mustafa M., Tabassum M., & Rahi M. (2021). Second law analysis of heat transfer in swirling flow of Bingham fluid by a rotating disk subjected to suction effect. *Thermal Science*, 25(1 Part A), 13–24.
5. Hafeez A., & Khan M. (2021). Flow of Oldroyd-B fluid caused by a rotating disk featuring the Cattaneo-Christov theory with heat generation/absorption. *International Communications in Heat and Mass Transfer*, 123, 105179.
6. Gul T., Bilal M., Alghamdi W., Asjad M. I., & Abdeljawad T. (2021). Hybrid nanofluid flow within the conical gap between the cone and the surface of a rotating disk. *Scientific Reports*, 11(1), 1–19. https://doi.org/10.1038/s41598-020-79139-8 PMID: 33414495

7. Jeon J., Park S., and Lee B. J., "Analysis on the performance of a flatplate volumetric solar collector using blended plasmonic nanofluid," Solar Energy, vol. 132, pp. 247–256, 2016.
8. Hussanan A., Salleh M. Z., Khan I., and Shafie S., "Convection heat transfer in micropolar nanofluids with oxide nanoparticles in water, kerosene and engine oil," Journal of Molecular Liquids, vol. 229, pp. 482–488, 2017.
9. Ghalambaz M., Doostani A., Izadpanahi E., & Chamkha A. J. (2020). Conjugate natural convection flow of Ag–MgO/water hybrid nanofluid in a square cavity. *Journal of Thermal Analysis and Calorimetry*, 139 (3), 2321–2336.
10. Motlagh S. Y. and Soltanipour H., "Natural convection of al2o3-water nanofluid in an inclined cavity using buongiorno's two-phase model," International Journal of Thermal Sciences, vol. 111, pp. 310–320, 2017.
11. Acharya N., Bag R., & Kundu P. K. (2019). Influence of Hall current on radiative nanofluid flow over a spinning disk: a hybrid approach. *Physica E*: *Low-dimensional Systems and Nanostructures*, 111, 103–112.
12. Akbar N. S., Raza M. and Ellahi R. (2015). Influence of induced magnetic field and heat flux with the suspension of carbon nano-tubes for the peristaltic flow in a permeable channel. Journal of Magnetism and Magnetic Materials, 381, 405415.
13. Shah N. A., Animasaun I. L., Chung J. D., Wakif A., Alao F. I., & Raju C. S. K. (2021). Significance of nanoparticle's radius, heat flux due to concentration gradient, and mass flux due to temperature gradient: The case of Water conveying copper nanoparticles. *Scientific Reports*, 11(1), 1–11. https://doi.org/10.1038/s41598-020-79139-8 PMID: 33414495
14. Sowmya G., Gireesha B. J., Animasaun I. L., & Shah N. A. (2021). Significance of buoyancy and Lorentz forces on water-conveying iron (III) oxide and silver nanoparticles in a rectangular cavity mounted with two heated fins: heat transfer analysis. *Journal of Thermal Analysis and Calorimetry*, 1–16.
15. Zhou S. S., Bilal M., Khan M. A., & Muhammad T. (2021). Numerical Analysis of Thermal Radiative Maxwell Nanofluid Flow Over-Stretching Porous Rotating Disk. *Micromachines*, 12(5), 540. https://doi.org/10.3390/mi12050540 PMID: 34068521
16. Patil A. (2016). A Modification and Application of Parametric Continuation Method to Variety of Nonlinear Boundary Value Problems in Applied Mechanics.
17. Shuaib M., Shah R. A., & Bilal M. (2020). Variable thickness flow over a rotating disk under the influence of variable magnetic field: An application to parametric continuation method. *Advances in Mechanical Engineering*, 12(6), 1687814020936385.
18. Shuaib M., Shah R. A., Durrani I., & Bilal M. (2020). Electrokinetic viscous rotating disk flow of Poisson-Nernst-Planck equation for ion transport. *Journal of Molecular Liquids*, 113412.
19. Wang Z., Liang S., Molnar C. A., Insperger T., & Stepan G. (2020). Parametric continuation algorithm for time-delay systems and bifurcation caused by multiple characteristic roots. *Nonlinear Dynamics*, 1–13.
20. Ahmadian A., Bilal M., Khan M. A., & Asjad M. I. (2020). Numerical analysis of thermal conductive hybrid nanofluid flow over the surface of a wavy spinning disk. *Scientific reports*, 10(1), 1–13. https://doi.org/10.1038/s41598-019-56847-4 PMID: 31913322
21. Ma Y., Mohebbi R., Rashidi M. M. & Yang Z. MHD convective heat transfer of Ag-MgO/water hybrid nanofluid in a channel with active heaters and coolers. *Int. J. Heat Mass Transf.* 137, 714–726 (2019).
22. Shah N. A., Animasaun I. L., Wakif A., Koriko O. K., Sivaraj R., Adegbie K. S., et al. (2020). Significance of suction and dual stretching on the dynamics of various hybrid nanofluids: Comparative analysis between type I and type II models. *Physica Scripta*, 95(9), 095205.